Critical Regimes of Oscillatory Deformation of Polymeric Systems Above Glass Transition and Melting Temperatures

G. V. VINOGRADOV, A. I. ISAYEV, and E. V. KATSYUTSEVICH,
Institute of Petrochemical Synthesis of the USSR Academy of Sciences, Moscow, USSR

Synopsis

High molecular weight linear polymers and their concentrated solutions were investigated over a wide range of frequencies and amplitudes of oscillatory deformation. At definite critical deformation and stress amplitudes, the resistance to deformation drops abruptly as a result of the rupture of continuity of polymer specimens in the region of action of the highest shear stresses. The lowest critical values of deformation rate amplitudes are inversely proportional to the initial viscosity and correspond quantitatively to the critical shear rates at which the spurt occurs during the flow of polymeric systems in ducts. The spurt effect is due to the transition of the polymer systems to the forced high-elastic state, in which they behave like quasi-cured polymers whose deformability is always limited. Up to the critical values of the stress amplitudes, narrow-distribution high molecular weight linear flexible-chain polymers behave like Hookean bodies, whereas the broad-distribution polymers show a sharply defined nonlinear behavior which asymptotically passes to a spurt. The amplitude dependence of the dynamic characteristics of the high molecular weight linear polymers, as well as their non-Newtonian behavior, is due to polymolecularity. An increase in deformation amplitudes reduces the frequency at which the spurt, and hence the transition of the polymer systems to the high-elastic state, is observed. Therefore, under conditions of oscillatory deformation the physical state (fluid or high-elastic) is determined not only by the frequency but also by the value of deformation. In the high-elastic state region (estimated at low amplitude deformation), the critical deformation amplitude is frequency independent and has an unambiguous relationship with the molecular mass of the chain (M_e) between the entanglements. For the bulk polymers studied, the spurt in the high-elastic state occurs at stress amplitudes of the order of 10^5 N/m^2 irrespective of frequency, molecular mass, or polymolecularity. In concentrated polymer solutions, in the high-elastic state the critical stress amplitudes decrease with reducing polymer content, whereas the critical deformation amplitudes increase.

Introduction

At temperatures above the glass transition region, polymer systems may pass from the fluid to the forced high-elastic state by deformation. This is a relaxation transition, which occurs upon increase in deformation rates. It is of great importance because in the high-elastic state the deformability of polymer systems is always limited, which fact is most pronounced in narrow-distribution, high molecular weight linear polymers and their concentrated solutions. This limitation is lifted if one uses the method of small-amplitude oscillatory deformation. Then, with increasing frequencies it is possible not only to determine the conditions of transition from the terminal zone to the high-elasticity plateau, which is equivalent to transition from the fluid to the high-elastic state, but also to establish the length of the high-elasticity plateau on the frequency scale.

At high deformation one observes a complex of effects that are specifically

Journal of Applied Polymer Science, Vol. 22, 727–749 (1978)

0021-8995/78/0022-0727$01.00

associated with the deformation conditions. Thus, an increase in shear rates and stresses up to certain critical values during the polymer system flow in capillary ducts leads to a spurt effect, which may be attended by an increase in volume outputs by tens and thousands of times.[1–4]

In narrow-distribution, high molecular weight polymers non-Newtonian behavior manifests itself only slightly up to the spurt. If we assume for these polymers the shear rate–frequency equivalence, we will find, according to the results of experiments conducted in capillary viscometers, that the shear rates at which the spurt occurs are close to the frequency corresponding to the maximum of the frequency dependence on the loss modulus, while the critical shear stresses are close to the loss modulus at the point of maximum (small-amplitude deformation).

In uniaxial extension of narrow-distribution, high molecular weight polymers, critical values of deformation rates and stresses are achieved at which a specimen rupture occurs with a time-dependent ultimate strength.[5,6] The "spurt" effect, which is observed in capillary viscometers, and the specimen rupture in uniaxial extension are attributed[1–6] to the transition of the polymers to the forced high-elastic state and to their limited deformability in this state.

In the case of polydisperse polymers, on their small-amplitude cyclical deformation the transition from the terminal zone to the high-elasticity plateau is found to be greatly extended and the plateau to be inclined. In experiments on various viscometers, broad-distribution polymers have a wide range of non-Newtonian flow that terminates in asymptotic transition to a spurt.

In the light of the foregoing, of great interest is the transition from small to large shear deformations (within a wide frequency range) when one should expect effects similar to the spurt in capillaries and achievement of the ultimate strength of polymers in uniaxial extension, especially because it was previously observed that the shear deformation amplitudes greatly affect the dynamics of polymer systems.[7,8]

The main questions posed in the present paper are as follows: To what extent do large shear deformations affect the transition from the fluid to the forced high-elastic state, i.e., how is this transition shifted on the frequency scale? How is the limited deformability of polymer systems manifested upon increase in frequencies and oscillation amplitudes? How does the spurt effect manifest itself under conditions of cyclical deformation, and how do the critical parameters corresponding to it depend on the nature of the polymer systems and the molecular mass of the polymers?

EXPERIMENTAL

Method of Investigation

To investigate the critical regimes of cyclical deformation of polymer systems, a BP-72 vibrorheometer was used for which a diagram is presented in Figure 1. The device consists of the following principal parts: a working unit, a system for assigning forced harmonic oscillations, a torsion head, and a system for recording the parameters measured. The working unit is made in the form of two coaxial cylinders, 1 and 2. The coaxial arrangement of the cylinders is ensured by a system of supports. In the outer cylinder the support is a precision roll-

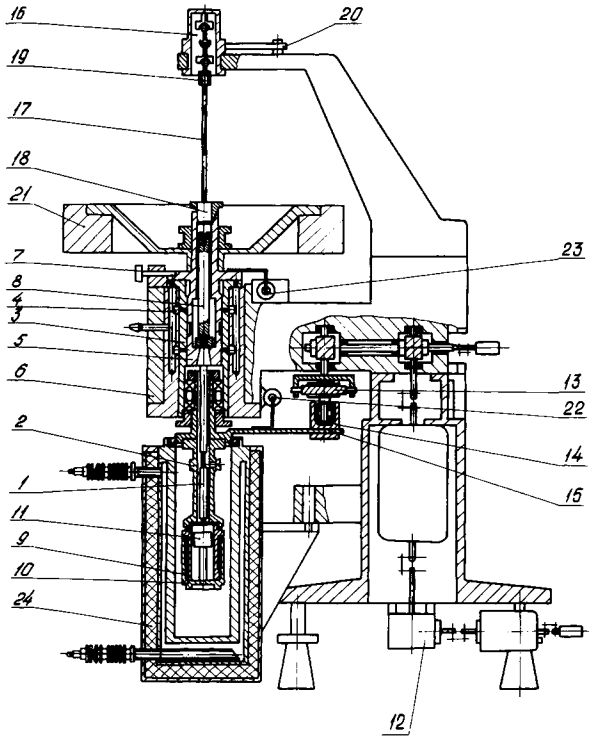

Fig. 1. Diagram of vibrorheometer BP-72. For key see text.

ing-friction bearing. In the inner cylinder use is made of an air radial-thrust bearing operating on compressed air, which is fed under a pressure not below 3×10^5 N/m^2. The air bearing consists of a stator (3), a nozzle (4) for feeding the air into the gap (1.5×10^{-5} M), and a rotor (5). The air bearing stator is pressed into a massive steel block (6). The block carries a lock (7), which serves to fix the zero position of the rotor and to prevent its vertical displacement together with the inner cylinder during the feeding of the working unit with the test substance. The inner cylinder contacts the air bearing rotor along a conical surface. A special nut (8) serves to tighten up the inner cylinder cone, and when it is released the inner cylinder is pushed out of the housing of the air-bearing rotor. Both the inner and outer cylinders are replaceable.

Filling of the working unit with the test substance is done with the aid of a filling device whose design is practically the same as the one described earlier[9] and which consists of a cylinder (9), a cap (10), and a piston (11).

Forced harmonic oscillations are assigned by means of three motors I–III (motor III is not shown in Fig. 1), a two-stage reducing worm gear (12), and an eccentric mechanism (13) which, together with the guide (14) and the lever (15), forms a link gear. The latter transforms the rotary motion of the motor into oscillatory motion of the outer cylinder. By switching on one motor or the other, it is possible to obtain the following frequencies: from the electric motor that is installed vertically and operates bypassing the reducing gear, 3–100 cps; from the electric motors operating through the reducing gear, in the first stage 6×10^{-2} to 2 cps and in the second stage 10^{-3} to 3×10^{-2} cps. Smooth frequency adjustment inside each range is ensured. The frequency is assigned with the aid

of a regulator connected to tachogenerators that are fastened to the motor shaft. The frequency is read off the scale of a milliammeter connected to the tachogenerator and set up on the external panel of the regulator.

The torsion head (16) is designed for fastening steel torsion bars (17) of different rigidity. One end of a torsion is fixed to the air bearing with the aid of a wedge (18), and the other, to a cardan suspension (19). The latter is attached to the head (16), which can be turned by an angle up to 6×10^{-2} rad by moving the lever (10) with a micrometric screw. The cardan suspension prevents the wedging of the air bearing during the fixing of the torsion bars. The inertia moment of the inner cylinder of the working unit is varied by loading the inner cylinder with a weight (21) that consists of replaceable discs or a rod with weights sliding along it. The inertia moment varies from 2.56×10^{-5} to 1.3 kg m^2.

The oscillations are recorded with the aid of two induction transducers (22 and 23) connected to the outer and inner cylinders of the working unit, respectively. The transducers are fed from an audio oscillator with a voltage of 6 V and a frequency of 2×10^4 cps. The signal from the transducers arrives at a loop oscillograph provided with a time marker and a device for automatic recording of the signal on ultraviolet photo paper.

The thermostating of the working unit is achieved with the aid of a heat exchanger (24) through which the liquid is pumped from the thermostat; it is filled with an intermediate heat transfer agent. The device housing has a hole in which the heat exchanger rod is fixed. The device is provided with two heat exchangers—water and oil—which ensure thermostating of specimens up to 200°C. The device is assembled on a tripod base with damping supports.

The test polymer is placed in the annular gap between the outer and inner cylinders. The outer cylinder of the working unit is assigned torsional oscillations with different frequencies and an increasing amplitude, and the amplitude of the motion of the inner cylinder suspended by the high-rigidity torsion rod (17) is recorded. This determines the amplitude of the torque due to the polymer deformation.

Of great importance for the purposes of this work is the possibility of disassembling the working unit during the deformation of the polymer systems. It would be expected that in the spurt regime the outer cylinder, together with the polymer being deformed, should readily separate from the inner cylinder. The possibility of such disassembly of the working unit during device operation was provided in the design.

Let the outer cylinder be assigned harmonic oscillations by the law

$$A = A_{OR} e^{i\omega t} \tag{1}$$

where A_{OR} is the oscillation amplitude (in rad), $\omega = 2\pi f$ is the circular frequency, f is the oscillation frequency, and t is the time. The equation of equilibrium with respect to the torques will then be written as

$$\tau \ddot{A}_r + cA_r - G^*(\gamma_R - \gamma_r) \cdot \frac{\pi h (R + r)^2}{2} = 0 \tag{2}$$

where τ is the inertia moment of the inner cylinder, $\ddot{A}_r$ is the acceleration on the inner cylinder, C is the torsion rod rigidity (modulus), A_r is the function determining the displacement of the inner cylinder in time, $G^* = G' + iG''$ is the complex shear modulus of the polymer systems, G' is the storage modulus, G''

is the loss modulus, h is the specimen height, R and r are, respectively, the radii of the outer and inner cylinders, γ_R and γ_r are the deformations determined by the motion of the outer and inner cylinders, respectively, calculated by the formulas

$$\gamma_R = \frac{A_R \cdot R}{R - r} \tag{3}$$

$$\gamma_r = \frac{A_r \cdot r}{R - r} \tag{4}$$

The first term of eq. (2) determines the torque due to the inertia of the inner cylinder, the second term determines the torque due to the torsion rod, and the third term determines the torque due to the deformation of the polymer system. The solution to eq. (2) will be sought in the form

$$A_r = A_{or} e^{i(\omega t + \delta)} \tag{5}$$

where δ is the phase shift in the motion of the inner cylinder with respect to the outer one due to the viscoelastic properties of the polymer and the inertia of the inner cylinder, and A_{or} is the oscillation amplitude of the inner cylinder.

Then, substituting eqs. (1), (3), and (4) and the solution (5) in eq. (2), we obtain the identity

$$-\tau\omega^2 e^{i\delta} e^{i\omega t} + cA_{or} e^{i\delta} e^{i\omega t} - G^* \left(\frac{RA_{OR} \cdot e^{i\omega t}}{R - r} - \frac{rA_{or} \cdot e^{i\delta} e^{i\omega t}}{R - r} \right) \cdot \frac{\pi h (R + r)^2}{2} = 0$$

Cancelling by $e^{i\omega t}$, we readily obtain the complex shear modulus:

$$G^* = \frac{2(c - \tau\omega^2) A_{or} (R - r) e^{i\delta}}{\pi h (R + r)^2 (RA_{OR} - rA_{or} e^{i\delta})} \tag{6}$$

Isolating the real and imaginary parts, we get the expression for the storage and loss moduli

$$G' = \frac{2(c - \tau\omega^2)(R - r) A_{or} (RA_{OR} \cos\delta - rA_{or})}{\pi h (R + r)^2 (R^2 A_{OR}^2 + r^2 A_{or}^2 - 2RrA_{OR}A_{or} \cdot \cos\delta)} \tag{7}$$

$$G'' = \frac{2(c - \tau\omega^2)(R - r) RA_{Or} A_{OR} \sin\delta}{\pi h (R + r)^2 (R^2 A_{OR}^2 + r^2 A_{oR}^2 - 2RrA_{OR}A_{or} \cdot \cos\delta)} \tag{8}$$

The stress amplitude arising in the polymer system is determined by

$$\tau_0 = |G^*| \gamma_0 = \frac{2(c - \tau\omega^2) \cdot A_{or}}{\pi h (R + r)^2} \tag{9}$$

The polymer deformation amplitude is determined by the formula of addition of harmonic oscillations:

$$\gamma_0 = \frac{(R^2 A_{OR}^2 + r^2 A_{or}^2 - 2RrA_{OR}A_{or} \cos\delta)^{1/2}}{R - r} \tag{10}$$

Thus, by making measurements at given values of frequency and amplitude, we determine the amplitude of stress τ_0 and deformation γ_0 from eqs. (9) and (10).

A polymer test in cyclical deformation with large amplitudes is carried out as follows. The outer cylinder is assigned harmonic oscillations with a constant frequency and an increasing oscillation amplitude. The oscillations of the outer and inner cylinders are photorecorded. The amplitudes A_{OR} and A_{or}, the frequency ω, and the phase shift δ are determined from the photorecording. Then, eqs. (9) and (10) are used to calculate the stress and deformation amplitudes. Such measurements are carried out at frequencies from 10^{-3} to 10^{2} cps and oscillation amplitudes from 1.8×10^{-3} to 3.5×10^{-2} rad. To ensure a high uniformity of the shear stress field, use is made of the annular gap formed between the outer and inner cylinders of radius 5×10^{-3} and 4.75×10^{-3} m, respectively, with the height of the working surface 2×10^{-2} and 5×10^{-2} m. Under these conditions, at an oscillation amplitude of 3.5×10^{-2} rad, it is possible to achieve the maximum value of the deformation amplitude, which is equal to 80%. To increase the maximum deformation assigned to the polymer up to 180%, use is made of a working unit with radii of the inner and outer cylinders of 1.475×10^{-2} and 1.5×10^{-2} m, respectively, the height of the working surface being 5×10^{-3} m. In some cases, when it is necessary to achieve a deformation amplitude of 300%, use is made of a working unit with radii of the inner and outer cylinders 2.975×10^{-2} and 3×10^{-2} m, respectively, the height of the working surface being 5×10^{-3} m. To eliminate the bottom effect, the polymer is cut flush with the end face of the inner cylinder. Torsion rods of length 2×10^{-1} m and diameter

TABLE I
Characteristics of Polymers Studied

Polymer no.	Polymer	Content, %	$M_w \times 10^{-5}$	M_w/M_n	Microstructure, %			
					cis-1,4	trans-1,4	1,2	3,4
1	2	3	4	5	6	7	8	9
1	Polybutadiene	100	0.76	1.2	45.0	45.0	10	—
2	Polybutadiene	100	1.41	1.10	47.2	44.0	8.8	—
3	Polybutadiene	100	2.30	1.10	45.2	45.6	9.2	—
4	Polybutadiene	100	3.2	1.10	45.0	46.0	9.0	—
5	Polybutadiene "Europrene"	100	2.63	3.0	79.0	14.0	7.0	—
6	Polyisoprene	100	1.48	1.61	72.0	20.8	—	6.2
7	Polyisoprene	100	2.40	1.14	77.4	14.6	—	8.0
8	Polyisoprene	100	3.80	1.10	79.0	15.2	—	5.8
9	Polyisoprene	100	5.75	1.02	69.0	25.0	—	6.0
10	Mixture:							
	Polybutadiene	80	0.76	1.20	45.0	45.0	10.0	—
	Polybutadiene	20	3.80	1.11	51.5	38.5	10.0	—
11	Mixture:							
	Polybutadiene	30	3.20	1.10	45.0	46.0	9.0	—
	Polyisoprene	70	3.80	1.10	79.0	15.2	—	5.8
12	Block copolymer:							
	Butadiene	30	3.50	—	49.0	46.0	5.0	—
	Isoprene	70			89.0	—	—	11.0
13	Polyethylene	100	0.89	1.1				
14	Polyethylene	100	2.12	1.1				
15	Polystyrene	100	10.0	1.1				
16	Polybutadiene	100	1.41	1.12	48.0	47.0	5.0	—
17	Polybutadiene	100	1.41	1.15	46.0	44.5	9.5	—
18	Polybutadiene	100	3.0	1.10	45.0	43.0	12.0	—
19	Polybutadiene	100	3.0	1.10	45.0	41.0	14.0	—

from 5×10^{-3} to 8×10^{-3} m are used in experiments, this ensuring a high rigidity of the measuring device and making it possible to vary it between 3×10^{1} to 1.5×10^{2} N m/rad.

Measurements of the dynamic characteristics of polymers at small amplitudes are also conducted with the aid of a VR-72 vibrorheometer in the frequency range of 10^{-3}–10^{2} cps, which uses various measurement methods in addition to the above-described ones, namely, the method of freely damping oscillations[10] in the frequency range of 10^{-1}–10 cps, the resonance method[8,11] (1–100 cps), and the method of stress assignment and deformation measurement[12] (10^{-3}–1 cps). The relative error in the determination of the storage and loss moduli does not exceed 16%. The combination of these measuring methods covers a wide frequency range.

Materials and Their Characteristics

The polymers investigated were polybutadienes (PB), polyisoprenes (PI), and one specimen of polystyrene (PS) synthesized by the method of anion polymerization on a Li-butyl catalyst. Also investigated were two fractions of narrow-distribution polyethylenes (PE) isolated from a broad-distribution linear polyethylene obtained on a chromium oxide catalyst.

It is important to note that the PB and PI specimens investigated were characterized by a narrow distribution and high molecular weights that were not lower than $10M_c$, where M_c is the molecular weight corresponding to a sharp increase in initial viscosity as related to molecular weight. Narrow distribution polymers were chosen that corresponded at 25°C to the terminal zone and the high-elasticity plateau upon small amplitude deformation in the frequency range of 10^{-3}–10^{2} cps.

Model binary mixtures of PB as well as mixtures of PB and PI were investigated. The mixtures were prepared by joint dissolution with subsequent isolation from the common solvent. The butadiene–isoprene block copolymer was investigated as a representative of block copolymers. To compare narrow- and broad-distribution polymers, use was made of polydisperse PE of the "Europrene" grade. A brief characterization of the polymers investigated is given in Table I. In addition to the specimens listed in the table, concentrated solutions of narrow-distribution PB were also investigated.

Dynamic Properties of Investigated Objects at Small Amplitudes

The data presented in Figure 2 refer to the range of small deformation amplitudes at which the components of the complex modulus are amplitude independent. In many cases, frequency dependences of the complex modulus components in the regions of the terminal zone and the high-elasticity plateau were obtained. The presence of a maximum of the loss modulus is worth mentioning whose height is independent of the molecular mass of the polymer but is different for PI and PB. The position of the maximum on the frequency axis (ω_{max}) is determined by the initial viscosity (η_0) of the polymers, namely, $\omega_{max} \propto \eta_0^{-1}$. An important feature of the function $G'(\omega)$ in narrow-distribution, high molecular weight polymers is the presence of a clearly defined high-elasticity plateau. The plateau height is practically independent of the molecular weight

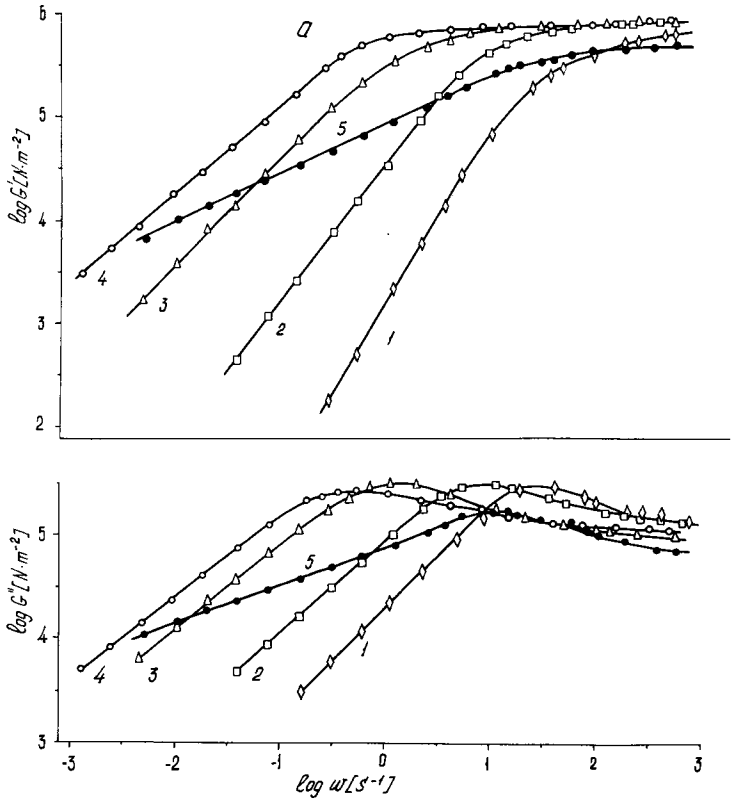

Fig. 2. Frequency dependence of storage (G') and loss (G'') moduli: (a) PB at 25°C; (b) PI at 25°C; (c) PE at 150°C, PS at 170°C, polymer mixture and block copolymer butadiene–isoprene at 25°C. Numbers at curves here and in Figs. 4, 5, and 7–9 correspond to polymer number in Table I. Solutions at 25°C: (d) PB-16 in methylnaphthalene; (e) PB-7 in diheptyl phthalate; (f) PB-18 in methylnaphthalene; (g) PB-18 in diheptyl phthalate. Numbers at curves in Figures 2(d)–2(g) correspond to weight contents of polymers in solution.

but is different for polymers of different nature. In contrast to the behavior of narrow-distribution PB, polydisperse PB of the "Europrene" grade is characterized by transition from the terminal zone to a high-elasticity plateau extending several decimal orders in frequency. The investigated polymer mixtures and also the copolymers show a clearly defined high-elasticity plateau and a slightly broadened maximum of the loss modulus. Concentrated solutions of PB are characterized by a decreased storage modulus on the high-elasticity plateau, G'_p, and a maximum of the loss modulus G''_{max}. With a decrease in polymer concentration in solution, the loss modulus maximum shifts toward the high frequencies. Here, the dependences established in reference 13 are confirmed, namely, $G'_p \propto C^2$, $G''_{max} \propto C^2$, where C is the polymer concentration in solution in weigh fractions.

RESULTS AND DISCUSSION

We begin by establishing the existence and nature of the manifestation of the critical regimes of cyclical deformation with large amplitudes. This must first of all show in the frequency range corresponding to the high-elastic state on

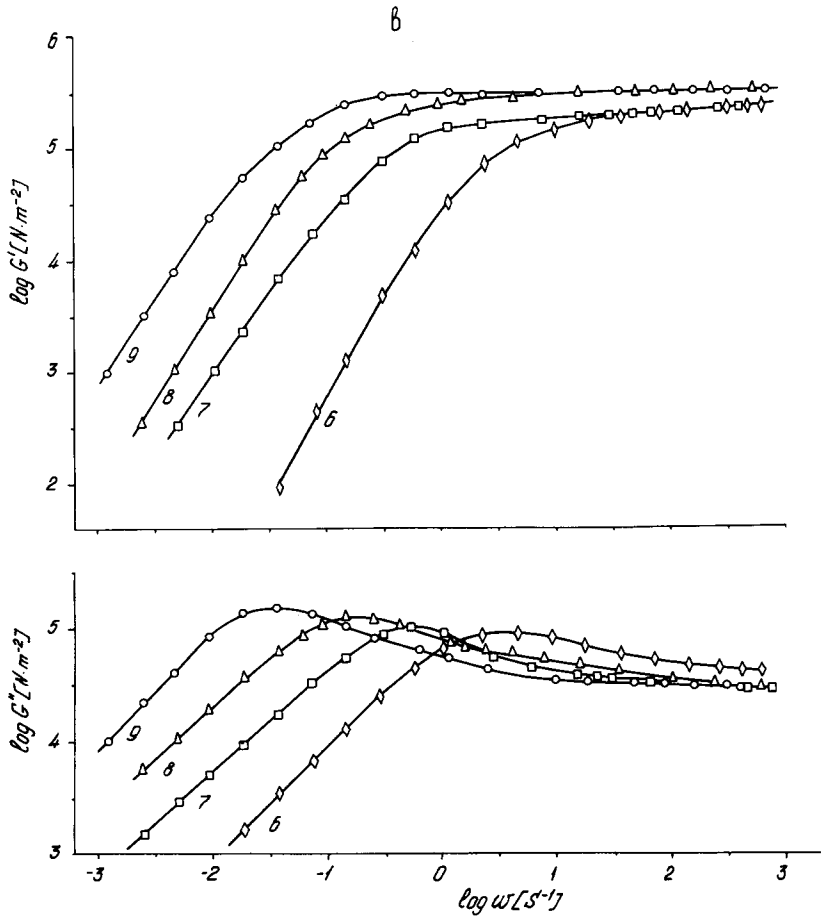

Fig. 2. (Continued from the previous page.)

small-amplitude deformation. Here, we proceeded from the facts that in experiments on capillary viscometers[1-4] the transition to the high-elastic state, in which the polymer deformability is always limited, corresponds to critical spurt regimes. In this connection, we staged experiments on a narrow-distribution, high molecular weight PB at a frequency of $\omega \gg \omega_{max}$, which corresponds to the high-elastic state under conditions of small-amplitude deformation and to the manifestation of the spurt effect in rotational devices.

To the critical deformation amplitude corresponds the critical stress amplitude, which is recorded from the abrupt decrease in torque; this is shown by the arrow in Figure 3(a). Up to the indicated critical values there is a linear relationship between the deformation and stress amplitudes, which is typical of narrow-distribution, high molecular weight specimens; the latter behave similarly to Hookean bodies in this respect.

From Figure 3(a) it follows that in large-amplitude cyclical deformations there is a spurt effect similar to the effect known from experiments on capillary viscometers. In experiments on capillary viscometers, however, the range of deformation rates corresponding to high elasticity cannot be investigated. Here, one can establish only the boundary of transition from the fluid to the high-elastic state, while in dynamic measurements on rotational devices small-amplitude

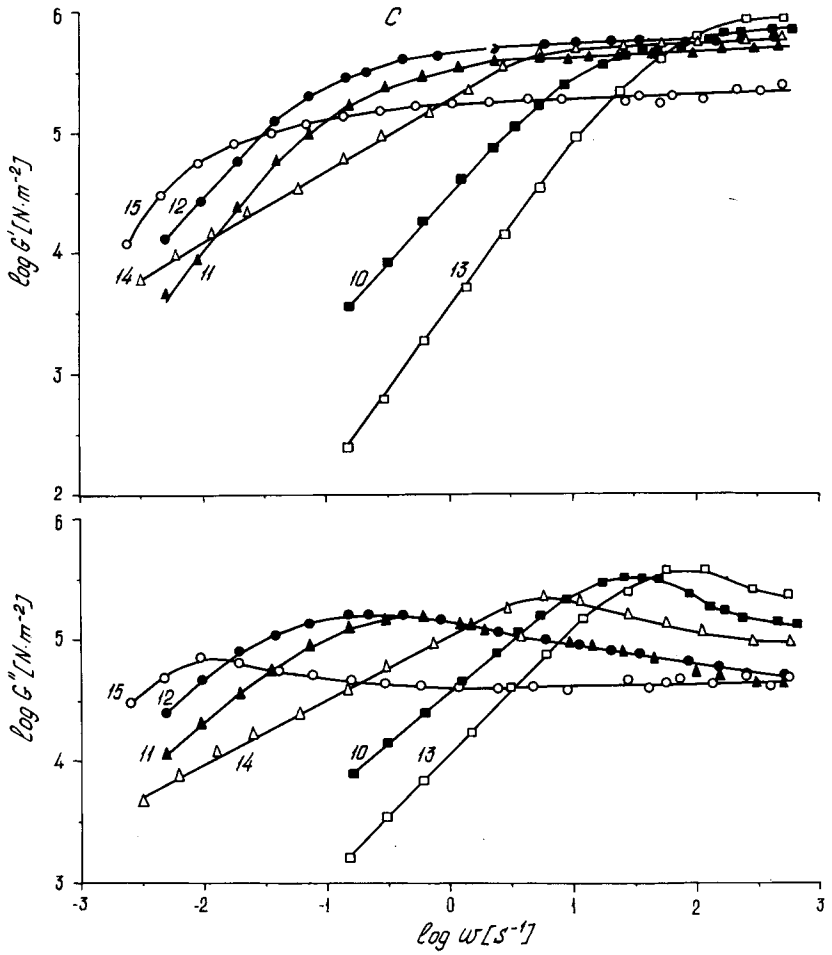

Fig. 2. (Continued from the previous pages.)

experiments in the region of the high-elastic state can be carried out. An important circumstance is that the critical regimes of cyclical deformation during a spurt in rotational instruments are independent of the degree of roughness of the working surfaces and the nature of the material that is in contact with the polymer. This can be regarded as an indirect indication that the cohesion rather than the adhesion effect is of greatest importance: the polymer rupture occurs in the most highly stressed region at the inner cylinder. This is confirmed by the fact that when disassembling the working unit in the spurt regime, the outer cylinder is readily removed together with the polymer. What happens during the spurt is also explained by the plots of Figure 3(b). We can see a strongly pronounced irregularity in time variation of stress, which is obviously associated with external friction and the processes of rupture and sticking of the polymer in the layers adjoining the inner cylinder. In the course of rupture the polymer is relaxed and it begins to stick to the inner cylinder. On passing to the stressed state, it suffers rupture, relaxes again, and so on.

A rather rapid recovery of the contact between the polymer and the inner cylnder in the course of relaxation after the deformation ceases is worth men-

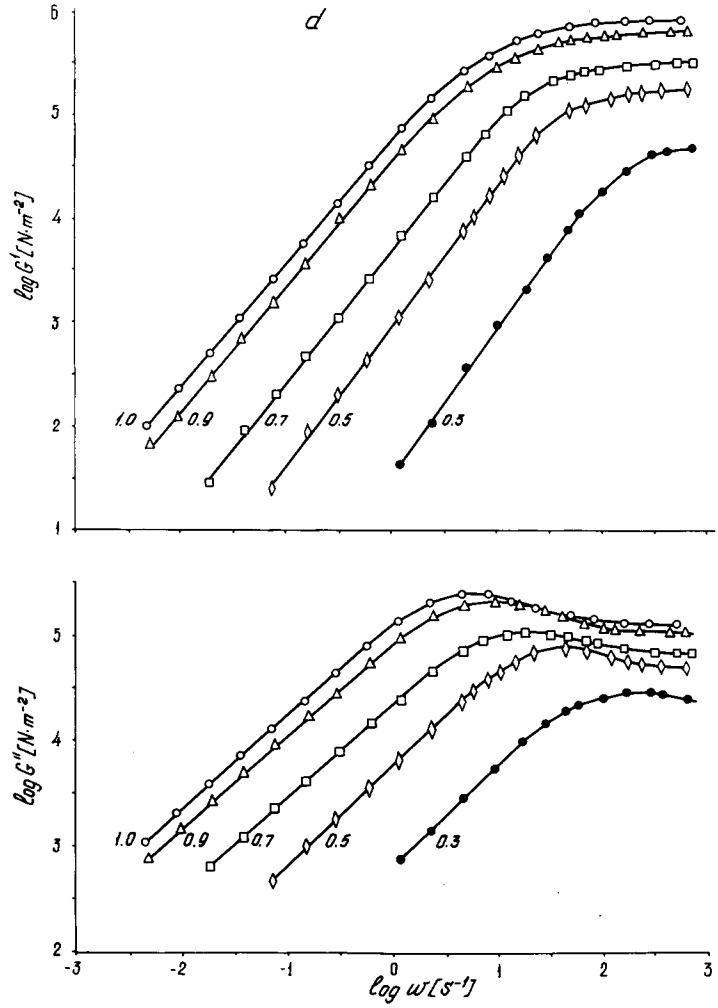

Fig. 2. (Continued from the previous pages.)

tioning. Thus, in the above-described experiment, after the spurt the initial value of the complex dynamic shear modulus in small-amplitude deformation is restored after only 26 sec of rest. It is possible that complete contact of the polymer with the inner cylinder is restored within shorter periods. But this was difficult to establish since transition to the small-amplitude deformation regime can take place only within a time of about 20 sec.

Of greatest importance is the question how the value of deformation affects the polymer transition from the fluid to the high-elastic state. The answer is supplied by the data presented in Figure 4 for a number of PB and PI specimens. The arrows on the x-axis indicate the values of ω_{max} obtained during small-amplitude deformation, which correspond under these conditions to the transition of the polymers from the fluid to the high-elastic state. At large amplitudes the criterion of this transition is a spurt. The plot of frequency dependence of the critical deformation amplitude ($\gamma_{0(cr)}$) corresponding to the spurt shows that a considerable increase in $\gamma_{0(cr)}$ is associated with a decrease by about one decimal order in the frequency corresponding to the transition in question. This

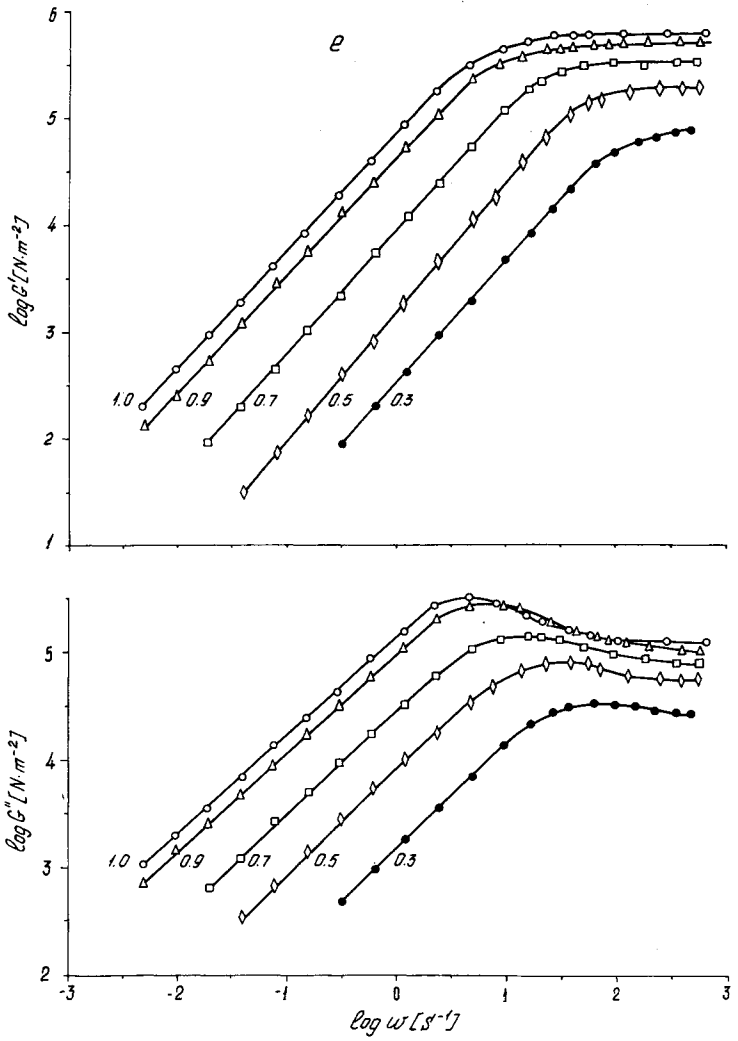

Fig. 2. (Continued from the previous pages.)

shift is greater for PB specimens (the upper plot), in which the value of $\gamma_{0(cr)}$ in the region of the high-elastic state is lower than in PI; this characterizes PB as more rigid polymers. In the frequency range $\omega > \omega_{max}$ the critical stress amplitudes $\tau_{0(cr)}$ are independent of the molecular mass of the specimens; they have the same values for PB and PI. The $\tau_{0(cr)}$ in PI is very close to the value of the critical spurt stress (τ_s) in capillary viscometers. In the case of PB the values of τ_s are about twice as high as those of the limiting values of $\tau_{0(cr)}$ obtained. This probably explains the twofold change in $\tau_{0(cr)}$ on transition from the frequency range corresponding to the fluid state to the high-elastic state (according to the data of small-amplitude deformation), although the reason is not yet clear.

The transition from the fluid to the high-elastic state is a relaxation process. Therefore, its rate characteristic plays the determining role. In this connection we shall introduce the concept of the critical amplitude of the deformation rate $\dot{\gamma}_{0(cr)} = \gamma_{0(cr)}\omega$. Accordingly, the data of Figure 4 are represented in Figure 5 in the form of the dependence of $\dot{\gamma}_{0(cr)}$ on ω. Here, as in the preceding figure,

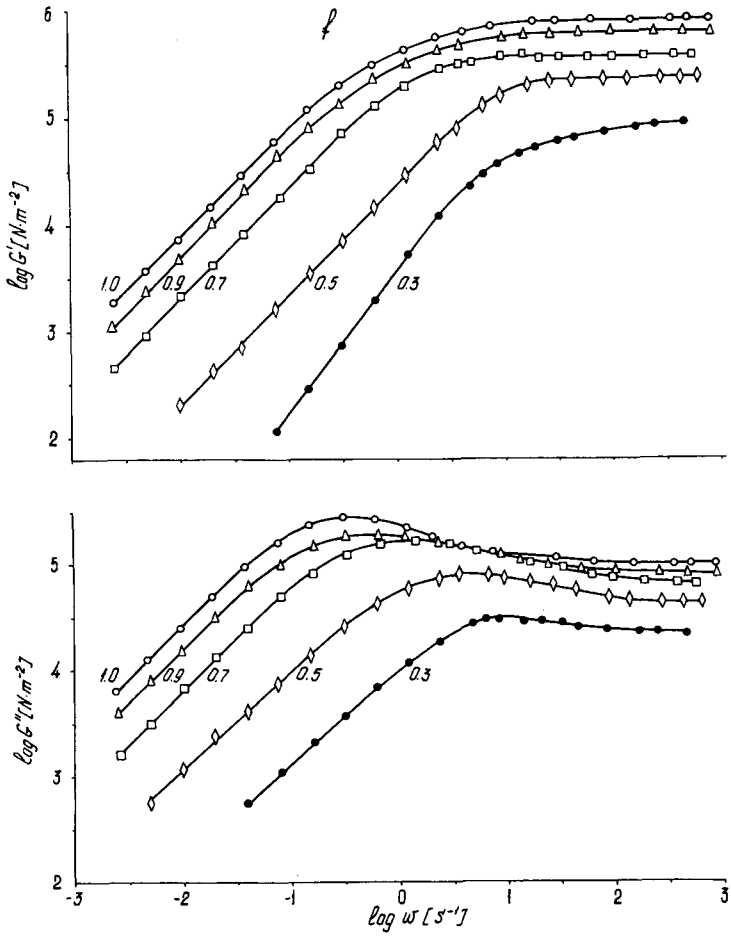

Fig. 2. (Continued from the previous pages.)

the arrows on the x-axis show the values of ω_{max} for the corresponding polymers. The data presented in Figure 5 indicate that the transition from the fluid to the high-elastic state in the large-deformation range occurs, to a first approximation, at a value of $\dot{\gamma}_{0(cr)}$ constant for each given polymer that strongly depends on the molecular mass of the polymer.

It has been shown above that in the high-frequency range $\gamma_{0(cr)}$ = const. Accordingly, $\dot{\gamma}_{0(cr)}$ increases linearly with frequency, and this linear dependence is invariant with the molecular weight. Transition from deformation regimes when $\dot{\gamma}_{0(cr)}$ = const. to the regime $\dot{\gamma}_{0(cr)} \propto \omega$ occurs in a narrow range of frequencies close to ω_{max}.

It has been shown[1-4] that in the case of capillary viscometry a spurt takes place on attainment of a critical shear rate $\dot{\gamma}_s \propto \eta_0^{-1}$, or $M^{-3.5}$. Therefore, we shall compare the function $\dot{\gamma}_{0(cr)}(M)$ corresponding to the left-side horizontal portions on the curves in Figure 5 with the function $\dot{\gamma}_s(M)$ according to the data of reference 4. The results of the comparison are given in Figure 6, from which it can be seen that the dependences under discussion practically coincide. Hence, it follows that transition from the fluid to the high-elastic state occurs, qualitatively, in the identical way during the flow of polymers in capillaries and in large-amplitude cyclical deformation.

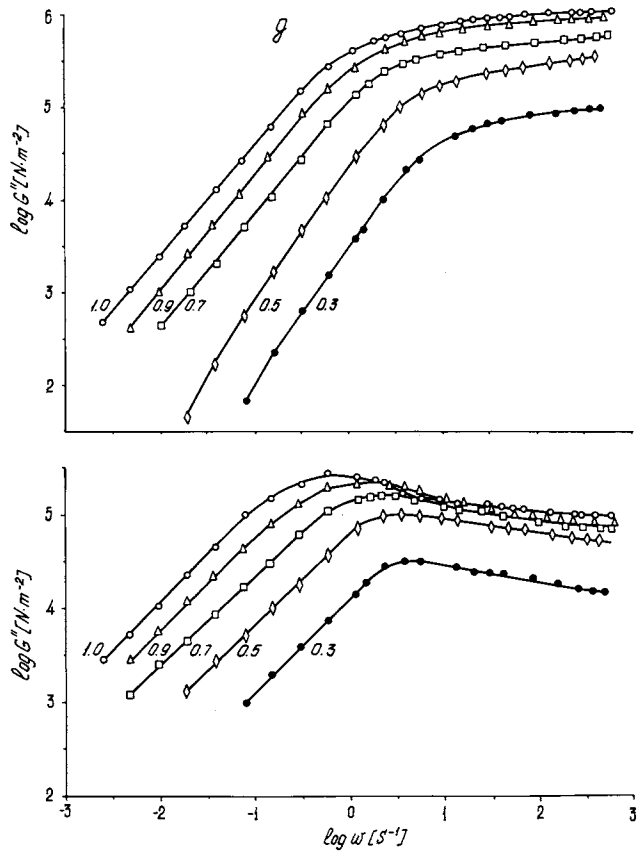

Fig. 2. (Continued from the previous pages.)

It has been noted above that at $\omega > \omega_{max}$ the value of $\gamma_{0(cr)}$ for PI specimens is higher than for PB. At the same time these polymers differ in the value of M_e (the molecular weight of the chain between the fluctuational entanglements), namely, it is 2.5 times higher for PI than for PB. Accordingly, the density of the entanglement network for PB is higher than for PI.[14,15] Therefore, the PI network can deform before the spurt occurs to higher amplitudes than the PB network. Thus, the result presented here indicate the presence of a clear-cut relationship between the conditions for attainment of the high-elasticity plateau of polymers and the existence of limiting critical regimes of large amplitude cyclical deformation. The foregoing suggests conditions for comparing the spurt for different polymers. Transition from the fluid to the forced high-elastic state and the spurt is determined under conditions of cyclical deformation by the value of $\dot{\gamma}_{0(cr)}$, whereas the spurt in the high-elastic state ($\omega \gg \omega_{max}$) is characterized by the value of $\gamma_{0(cr)}$, since under these conditions the value of the critical amplitude is frequency independent. The latter fact will be used by us when generalizing the data for different polymers.

Let us now consider the dependence $\tau_0(\gamma_0)$ for PB and PI of different molecular mass at different frequencies (Fig. 7). In the figure, the extreme right-hand points of all the curves correspond to the spurt, which is indicated by arrows for the upper curves. Some nonlinearity of the dependences $\tau_0(\gamma_0)$ at high values of τ_0 is evidently due to the unaccounted-for differences in the molecular weight

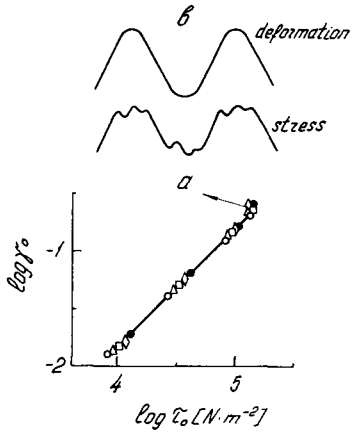

Fig. 3. (a) Dependence of stress amplitude on deformation amplitude of PB-4 at frequency of 20 cps and temperature 25°C. Working unit is made of steel; surfaces and ground torsion rods of different rigidity were used: (○) 1.43×10^2; (△) 8.25×10^1; (□) 3.01×10^1 Nm/rad; (●) working unit with inner cylinder having fluoroplast coating of thickness 15 μk; (◇) same with inner cylinder having 15 μk deep triangular notches spaced at 200 μk along generatrix; (b) typical photorecording of assigned deformation and stress arising in spurt regime.

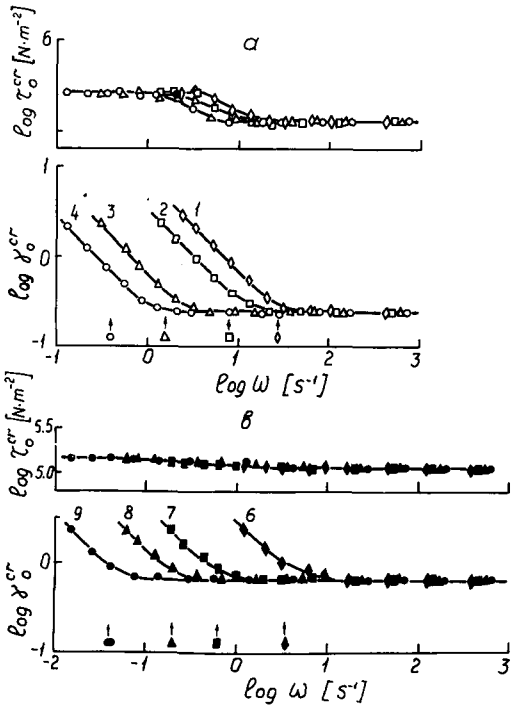

Fig. 4. Frequency dependences of critical stress and deformation amplitudes for PB (a) and PI (b) at 25°C. Arrows on x-axis indicate frequencies corresponding to ω_{max}.

distribution of the specimens. As regards the condition for the occurrence of the spurt itself, at high deformation frequencies and amplitudes $\gamma_0 > \gamma_{0(cr)}$, the amplitude of the torque falls away more abruptly than at low frequencies. These effects, however, are of secondary importance for the characteristics of the spurt

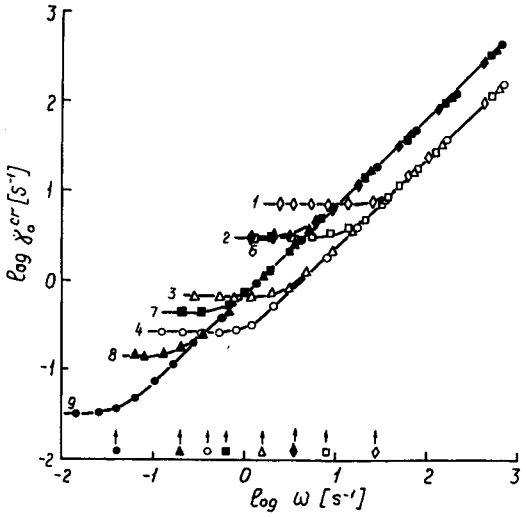

Fig. 5. Frequency dependence of critical amplitude of deformation rate for PB and PI at 25°C. Arrows on x-axis indicate frequencies corresponding to ω_{max}.

process, and the main parameters determining the spurt are the critical values of the deformation amplitudes, deformation rate, and stress.

We shall now discuss the limiting critical regimes of deformation of narrow-distribution PB mixtures. Since at $M \gg M_e$ the values of $\gamma_{0(cr)}$ and $\tau_{0(cr)}$ are independent of M, the critical parameters of mixtures must be independent of their composition. This is confirmed by the data of Figure 8 (curves 10). Quite a different picture is presented by the dependence $\tau_0(\gamma_0)$ and the conditions for the development of the spurt in broad-distribution PB, which contains low molecular weight fractions. It is seen from Figure 8 (curves 5) that the dependence $\tau_0(\gamma_0)$ is not only nonlinear over a wide range of parameters, but also that the spurt is attained asymptotically in the range of stress amplitudes practically independent of γ_0 at high frequencies. The assignment of high frequencies and large amplitudes may result in heating of the polymer, which must lead to a decrease in τ_0 at a given value of γ_0. Direct measurement of the polymer temperature in the gap at a frequency of 100 cps and at a maximum deformation amplitude of 180% has shown that in this deformation regime the temperature increases by not more than 6°C. It must be remembered, however, that the deformation frequencies mentioned above, see Figure 2(a), correspond to the high-elastic state. Therefore, simple calculation shows that the indicated temperature increase may merely lead to a slight reduction in the value of τ_0, whereas the experimental stress amplitude during the spurt decreases more than threefold.

The foregoing permits us to consider the nonlinear behavior of polymer systems in cyclical deformation with an increasing amplitude in the same way as was suggested for explanation of the non-Newtonian behavior of polydisperse polymers.[16] With an increase in amplitude (at the corresponding frequencies) the high molecular weight components pass over to the high-elastic state and behave like a filler, i.e., they do not show any fluidity themselves. Therefore, with an increase in deformation rate amplitude, the resistance to deformation increases more slowly because the dissipation losses in the high molecular weight

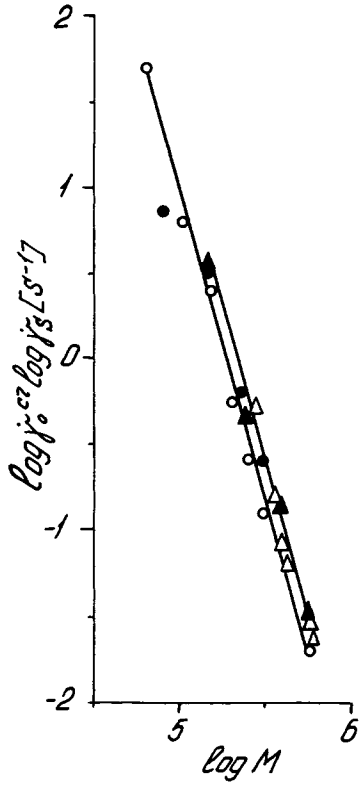

Fig. 6. Dependences of critical amplitude of deformation rate $\dot{\gamma}_{0(cr)}$ solid symbols and critical deformation rate $\dot{\gamma}_s$ (open symbols) on polymer molecular mass at 25°C: (●, ○) PB; (▲, △) PI. Values of $\dot{\gamma}_s$ are from reference 4.

component decreases. On further increase in deformation amplitude, an ever-increasing number of components pass over to the high-elastic state, the nonlinearity increases, and the rate of increase in stress amplitude slows down more and more unil finally most of the polymer passes to the high-elastic state and a spurt occurs. Thus, the nonlinear behavior of polymer systems in large-amplitude cyclical deformation is due to their polymolecularity, as in conditions of flow in capillaries.

The viscous and dynamic properties of mixtures of PB and PI and the block butadiene–isoprene copolymer have been studied.[17] It was shown that during the flow of these systems in capillaries, as in the case of homopolymers, a spurt occurs, and the critical shear rate $\dot{\gamma}_s$ of the copolymer is lower than for a mixture of the corresponding composition. Therefore, it was interesting to compare the behavior of the mixture and the copolymer with the same composition in large-amplitude cyclical deformation. The results of these investigations, given in Figure 8, show that for the block copolymer (curves 12) and a mixture (curves 11) of the corresponding composition it is possible to achieve critical regimes of cyclical deformation in the same way as was described for homopolymers. The critical parameters characterizing the regimes of cyclical deformation of the mixture do not differ from the critical parameters of narrow-distribution PI, which is due to its high content in the mixture (70%) and to its compatibility with PB.[17] The critical regimes of cyclical deformation of two-component systems,

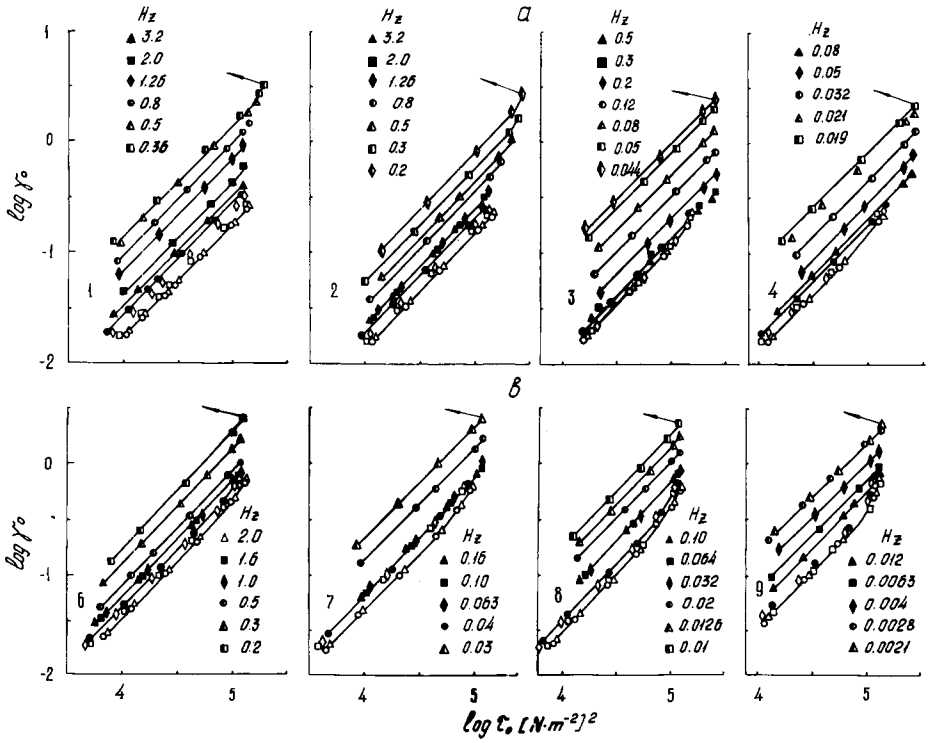

Fig. 7. Dependences of stress amplitude on deformation amplitude for narrow-distribution PB (a) and PI (b) at 25°C. Oscillation frequencies in cps are indicated at the graph field, except: (○) 100; (△) 50; (□) 20; (◇) 10; (●) 5.

however, must change substantially if the components form block copolymers. From the comparison of the data obtained on mixtures and a block copolymer (Fig. 8) it can be seen that the critical deformation amplitude of the block copolymer takes on an intermediate value between $\gamma_{0(cr)}$ of the PB–PI and PB–PB mixtures, whereas $\tau_{0(cr)}$ for the mixtures and the block copolymer coincide.

The spurt effect in cyclical deformation is just as characteristic of high molecular weight thermoplast melts. Figure 9 shows the dependences of the stress amplitude τ_0 on the deformation amplitude γ_0 for specimens PE-13 (right-hand curve 13), PE-14 (two curves 14 located on the left, next to curve 13), and specimen PS (two curves 15). The deformation of these polymers occurred at frequencies $\omega > \omega_{max}$. In the case of specimen PE-13, however, the frequencies used were near ω_{max}, see Figure 2(c), which explains some difference in the behavior of specimens PE-13 and 14, see Figure 9. It should be noted that the values of $\gamma_{0(cr)}$ for the specimen of high molecular weight PE and of PS differ more than threefold, while their values of $\tau_{0(cr)}$ differ only slightly.

In reference 13 it was found when studying PB solutions that in the case of high shear stresses concentrated solutions can pass over from the fluid to the forced high-elastic state, which manifests itself in the form of a flow spurt, as in the case of the nonplasticized polymer. From the data presented in Figure 10 it follows that in cyclical deformation of PB solutions the spurt effect is manifested in the way described above when discussing bulk polymers. Besides, a decrease in polymer concentration leads to the nonlinear relationship $\tau_0(\gamma_0)$ at

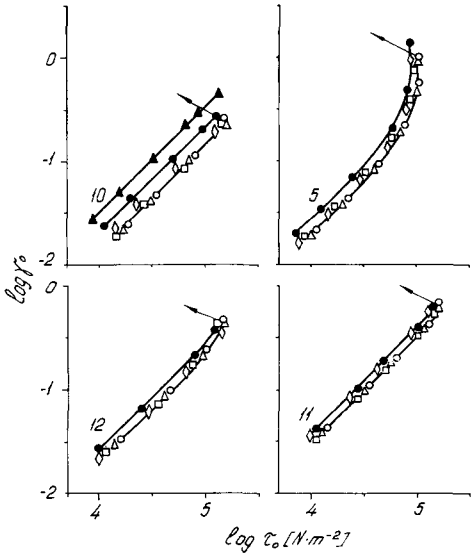

Fig. 8. Dependences of stress amplitude on deformation amplitude for mixtures: PB-PB (curves 10), PB-PI (curves 11), PB "Europrene" (curves 5), butadiene–isoprene block copolymer (curves 12) at 25°C. Frequency, in cps: (○) 100; (△) 50; (□) 20; (◇) 10; (●) 5; (▲) 2.

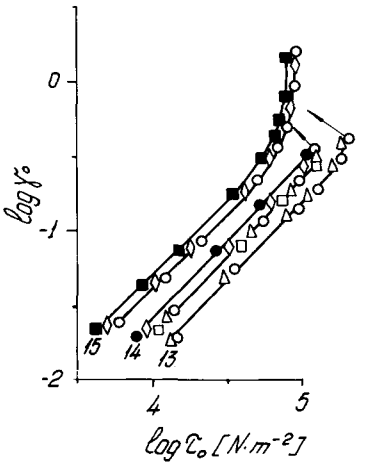

Fig. 9. Dependences of stress amplitudes on deformation amplitude for PE at 150°C (curves 13 and 14) and PS at 170°C (curves 15). Frequency, in cps: (○) 100; (△) 50; (□) 20; (◇) 10; (●) 5; (■) 1.

high stress amplitudes long before the spurt occurs. This effect is similar to what was observed in reference 13, where the decrease in polymer concentration in solution enhanced the non-Newtonian behavior of the system. At $\omega \gg \omega_{max}$, the values of $\tau_{0(cr)}$ and $\gamma_{0(cr)}$ are practically independent of the frequency and nature of the solvent. It is well known[18] that the solvent nature does not affect the viscoelastic properties of solutions of flexible-chain polymers. It should be noted that the frequency dependence of the parameters $\tau_{0(cr)}$ and $\gamma_{0(cr)}$ is manifested only at $\omega \to \omega_{max}$.

We now follow up the variation in the critical values of the stress and deformation amplitudes in relation to the polymer concentration in solution. The

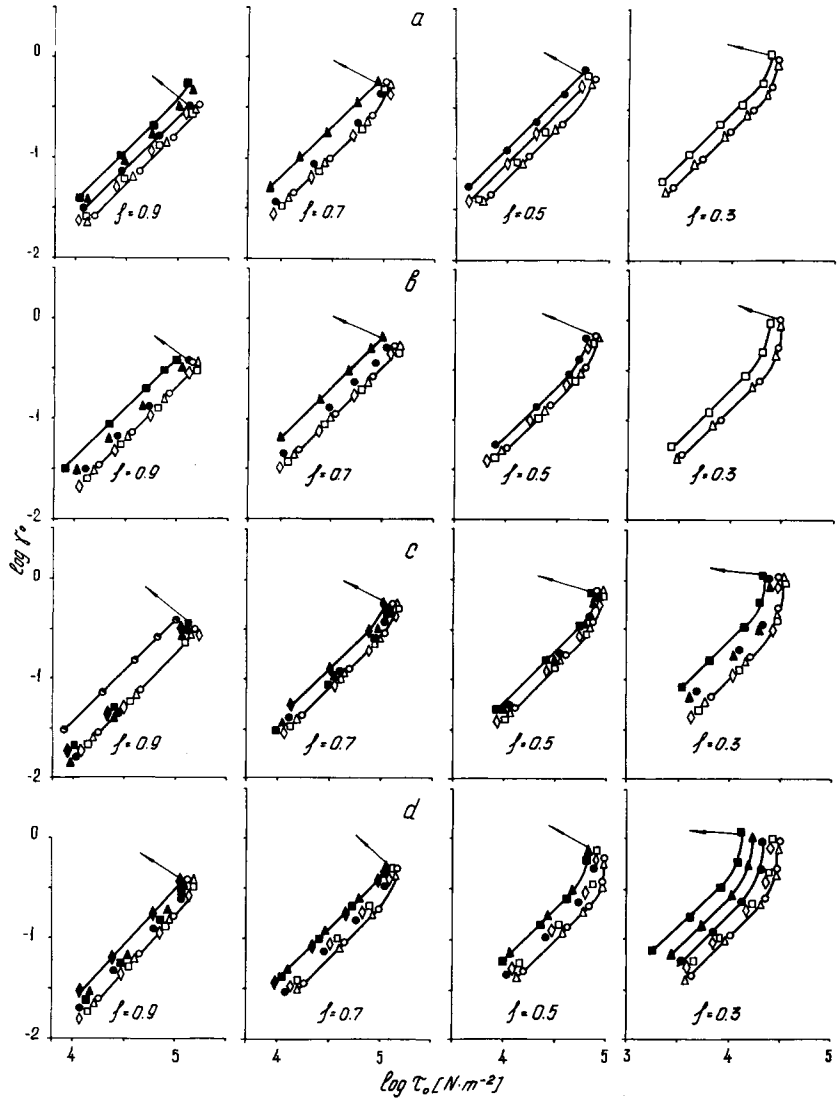

Fig. 10. Dependences of stress amplitude on deformation amplitude for PB solutions at 25°C: (a) PB-16 in methylnaphthalene; (b) PB-17 in methylnaphthalene; (c) PB-18 in diheptyl phthalate; (d) PB-19 in diheptyl phthalate. Frequency, in cps: (○) 100; (△) 50; (□) 20; (◇) 10; (●) 5; (▲) 2; (■) 1; (◆) 0.5; (◓) 0.2. Numbers at curves correspond to weight content of polymer in solution.

indicated dependences, plotted on the basis of experimental data, are depicted in Figure 11. In plotting these, use was made of the values of $\gamma_{0(cr)}$ and $\tau_{0(cr)}$ obtained at sufficiently high frequencies, where the critical parameters are frequency independent. It is easy to see from Figure 11 that with an increase in polymer concentration in solution the critical parameters $\tau_{0(cr)}$ and $\gamma_{0(cr)}$ vary in opposite directions, namely, $\tau_{0(cr)}$ increases, whereas $\gamma_{0(cr)}$ decreased. The obtained augmentation of increasing critical stress amplitude with increasing polymer concentration is due to the reinforcement of the fluctuation entanglement network in solution and is in good agreement with the results of reference 13, where it was found that during the flow of PB solutions in capillaries the value

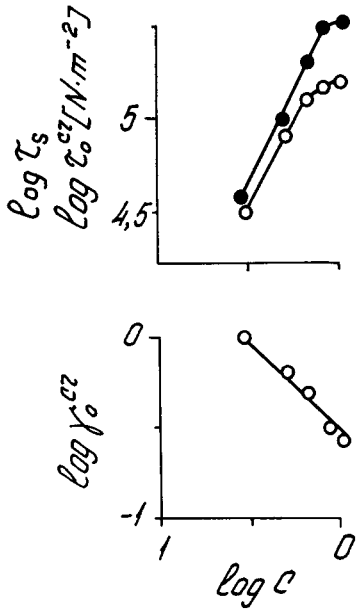

Fig. 11. Concentration dependences of critical stress amplitude $\tau_{0(cr)}$ (open symbols), shear stress τ_s (solid symbols), and deformation amplitude $\gamma_{0(cr)}$ for PB solutions in methylnaphthalene and diheptyl phthalate at 25°C. Data on τ_s are from reference 13.

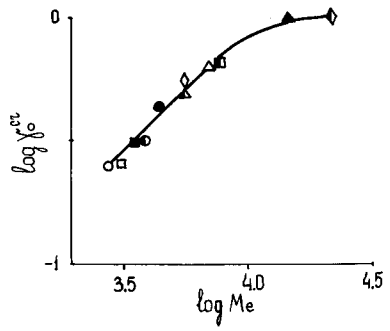

Fig. 12. Dependences of critical deformation amplitude on molecular weight of dynamic segment M_e for different polymer systems: (○) PB (25°C); (△) PI (25°C); (□) PB–PB mixture; (◇) PB–PI mixture (25°C); (●) butadiene–isoprene block copolymer (25°C); (▲) PS (170°C); (■) PE (150°C); PE solutions (25°C); (◐) 90 wt %; (▲) 70; (◧) 50; (◆) 30.

of τ_s grows with polymer concentration. The increase in the critical values of deformation amplitudes as the polymer concentration in solution decreases is due to the diminishing density of the fluctuation entanglement network owing to which the ability for developing deformation increases, and a spurt occurs at higher deformations.

As indicated above, the critical deformation amplitude in the high-elastic state ($\omega \gg \omega_{max}$) is independent of the molecular weight of the polymer if $M \gg M_e$ but depends on the value of M_e. The value of M_e for polymers and their solutions will be determined by the formula of the kinetic theory of rubber elasticity, $M_e = \rho RT/G'_p$, where ρ is the polymer or solution density, R is the universal gas constant, T is the absolute temperature, and G'_p is the value of the storage

modulus on the high-elasticity plateau. This formula has been obtained for cured rubbers possessing a stable network of chemical bonds.[19] In the present investigation, the equation for M_e is applied to the high-elastic state of uncured polymer systems, as was repeatedly suggested in references 1, 20, and 21. According to the data obtained it is possible to compile the following series of M_e values for bulk polymers: 2800, 3500, 4500, 7000, and 18000, and the following $\gamma_{0(cr)}$ values: 0.25, 0.3, 0.43, 0.6, and 1.0, respectively, for PB and PE and block copolymer of butadiene–isoprene, PI, and PS. The following series of M_e values has been obtained for the PB solutions investigated: 3200, 6300, 8000, and 28000, respectively, for polymer concentrations of 0.9, 0.7, 0.5, and 0.3 in solution.

We now pass over to joint consideration of the experimental values of $\gamma_{0(cr)}$ obtained for the investigated narrow-distribution polymers and their solutions. We shall plot the dependence of their values of $\gamma_{0(cr)}$ on the molecular mass of the dynamic segment M_e. The dependence obtained is presented in Figure 12. It follows that in the range of low M_e for the polymers and their solutions at hand there exists a power dependence of $\gamma_{0(cr)}$ on M_e. A further increase in M_e results in independence of $\gamma_{0(cr)}$ on M_e.

The curve shown in Figure 12 is the limiting deformation curve for oscillatory deformation of flexible-chain polymers in the high-elastic state. Beneath this curve is the region of stable oscillatory deformation, and above it is the region of unstable oscillatory deformation in which the spurt effect occurs. Thus, the deformability of polymers and their solutions in the high-elastic state is determined unambiguously by the value of the molecular weight of the dynamic segment, which depends on the value of the storage modulus on the high-elasticity plateau.

Investigation of high molecular weight specimens of PB, PI, PS, and linear PE shows that the values of $\gamma_{0(cr)}$ lie in a very narrow frequency range corresponding to the high-elastic state. This applies both to narrow- and broad-distribution polymers and also to two-phase mixtures of PB and PI and their block copolymers. Only the introduction of a solvent can decrease the value of $\gamma_{0(cr)}$, just as the height of the high-elasticity plateau decreases on reduction of the polymer concentration in solution. The narrowness of the range of $\tau_{0(cr)}$ values for the polymers investigated suggests that the value of Z_e, which represents the number of monomer units contained in the segment, exerts the determining effect.[22]

References

1. G. V. Vinogradov, *Pure Appl. Chem.*, **26**, 423 (1971); *ibid.*, **39**, 115 (1974); W. K. Schowalter, Ed., *Progress in Heat and Mass Transfer*, Vol. 5, Pergamon Press, Oxford, 1972, p. 51.

2. G. V. Vinogradov, *Rheol. Acta*, **12**, 357 (1973); *Pure Appl. Chem., Macromol. Chem.*, **8**, 413 (1973).

3. G. V. Vinogradov, N. I. Insarova, V. V. Boiko, and E. K. Borisenkova, *Polym. Eng Sci.*, **12**, 523 (1972).

4. G. V. Vinogradov, A. Y. Malkin, Y. G. Yanovsky, E. K. Borisenkova, B. V. Yarlykov, and G. V. Berezhnaya, *J. Polym. Sci., Phys. Ed.*, **10**, 1061 (1972).

5. G. V. Vinogradov, *Rheol. Acta*, **14**, 942 (1975).

6. G. V. Vinogradov, A. Y. Malkin, V. V. Volosevich, V. P. Shatalov, and V. P. Yudin, *J. Polym. Sci., Phys. Ed.*, **13**, 1721 (1975).

7. W. Philippoff, *Trans. Soc. Rheol.*, **10**, 317 (1966).

8. G. V. Vinogradov, Y. G. Yanovsky, and A. I. Isayev, *J. Polym. Sci. A-2*, **8**, 1239 (1970).

9. I. M. Belkin, G. V. Vinogradov, and A. I. Leonov, *Rotational Instruments. Measurements*

of Viscosity and Physico-Mechanical Properties of Materials (in Russian), Mashinostroyeniye, Moscow, 1968.

10. S. I. Sergeyenkov and Y. G. Yanovsky, *Zavodsk. Lab.*, **37**, 614 (1971).
11. H. Markoviz, *J. Appl. Phys.*, **23**, 1070 (1952).
12. J. L. den Otter, *Rheol. Acta*, **8**, 355 (1969).
13. N. K. Blinova, S. I. Sergeyenkov, A. Y. Malkin, Y. G. Yankovsky, and G. V. Vinogradov, *Mekh. Polim.*, **1**, 132 (1973).
14. J. T. Gruver and G. Kraus, *J. Polym. Sci.*, **A-2**, 797 (1964).
15. L. J. Fetter, *Res. Natl. Bur. Stand.*, **A-69**, 145 (1965).
16. A. Y. Malkin, N. K. Blinova, G. V. Vinogradov, M. P. Zabugina, O. Y. Sabsai, V. G. Shalganova, I. Y. Kirchevskaya, and V. P. Shatalov, *Eur. Polym. J.*, **10**, 445 (1974).
17. Nguen-Vin-Chiy, A. I. Isayev, A. Y. Malkin, C. V. Vinogradov, and I. Y. Kirchevskaya, *Vysokomol. Soedin.*, **17A**, 855 (1975).
18. V. E. Dreval, A. Y. Malkin, G. V. Vinogradov, and A. A. Tager, *Eur. Polym. J.*, **9**, 85 (1973).
19. L. Treloar, *The Physics of Rubber Elasticity*, Oxford, 1949.
20. R. Porter and J. Johnson, *Chem. Rev.*, **66**, 1 (1966).
21. G. V. Vinogradov, E. A. Dzyura, A. Y. Malkin, and V. A. Grechanovsky, *J. Polym. Sci. A-2*, **9**, 1153 (1971).
22. W. Graessley, The Entanglement Concept in Polymer Rheology, in *Advances in Polymer Science*, Vol. 16, Springer-Verlag, Berlin, 1974.

Received March 24, 1977